Electrically injected GaAsBi/GaAs single quantum well laser diodes

Downloaded from: https://research.chalmers.se, 2024-03-20 08:29 UTC

Citation for the original published paper (version of record):

Liu, J., Pan, W., Wu, X. et al (2017). Electrically injected GaAsBi/GaAs single quantum well laser diodes. AIP Advances, 7(11): Article Number: 115006 -. http://dx.doi.org/10.1063/1.4985231

N.B. When citing this work, cite the original published paper.

research.chalmers.se offers the possibility of retrieving research publications produced at Chalmers University of Technology.
It covers all kind of research output: articles, dissertations, conference papers, reports etc. since 2004.
research.chalmers.se is administrated and maintained by Chalmers Library

(article starts on next page)

AIP ADVANCES **7**, 115006 (2017)

Electrically injected GaAsBi/GaAs single quantum well laser diodes

Juanjuan Liu,[1,2] Wenwu Pan,[1,2] Xiaoyan Wu,[1,2] Chunfang Cao,[1]
Yaoyao Li,[1,b] Xiren Chen,[2,3] Yanchao Zhang,[1,4] Lijuan Wang,[1] Jinyi Yan,[1]
Dongliang Zhang,[1,2] Yuxin Song,[1] Jun Shao,[2,3] and Shumin Wang[1,5,a]
[1]*State Key Laboratory of Functional Materials for Informatics, Shanghai Institute of Microsystem and Information Technology, Chinese Academy of Sciences, Shanghai 200050, China*
[2]*School of Electronic, Electrical and Communication Engineering, University of Chinese Academy of Sciences, Beijing 100049, China*
[3]*National Laboratory for Infrared Physics, Shanghai Institute of Technical Physics, Chinese Academy of Sciences, Shanghai 200083, China*
[4]*School of Physical Science and Technology, ShanghaiTech University, Shanghai 200031, China*
[5]*Department of Microtechnology and Nanoscience, Chalmers University of Technology, Gothenburg 41296, Sweden*

(Received 27 May 2017; accepted 24 October 2017; published online 3 November 2017)

We present electrically injected GaAs/GaAsBi single quantum well laser diodes (LDs) emitting at a record long wavelength of 1141 nm at room temperature grown by molecular beam epitaxy. The LDs have excellent device performances with internal quantum efficiency of 86%, internal loss of 10 cm^{-1} and transparency current density of 196 A/cm^2. The LDs can operate under continuous-wave mode up to 273 K. The characteristic temperature are extracted to be 125 K in the temperature range of 77~150 K, and reduced to 90 K in the range of 150~273 K. The temperature coefficient of 0.3 nm/K is extracted in the temperature range of 77~273 K. © *2017 Author(s). All article content, except where otherwise noted, is licensed under a Creative Commons Attribution (CC BY) license (http://creativecommons.org/licenses/by/4.0/).*
https://doi.org/10.1063/1.4985231

INTRODUCTION

Bismuth (Bi)-containing GaAsBi is a promising candidate as an attractive gain medium for uncool telecommunication lasers. Incorporating a small amount of Bi into III-Vs can efficiently reduce the bandgap energy (88 meV/Bi% for GaAs$_{1-x}$Bi$_x$) resulting from the anti-crossing of the Bi impurity band with the GaAs valence band.[1] As the fraction of Bi in GaAsBi is up to 9%, the bandgap reaches 800 meV which matches up with 1.55 μm wavelength division multiplexing telecommunication systems.[2] The incorporation of Bi will increase the spin-orbit split energy, which will be larger than the bandgap when the Bi composition in GaAsBi is approximately up to 10%.[3] Therefore, the hot-hole induced Auger recombination and the inter-valence band absorption can be suppressed, resulting in the enhancement of luminous efficiency and characteristic temperature. Such processes may potentially decrease the electrical power wasted as heat in a 1.55 μm laser chip. In 2009, the 987 nm GaAsBi light emission diodes (LEDs) were demonstrated by Lewis *et al.*[4] The electroluminescence energy of the reported *p-i-n* LED was independent of temperature in the range of 100 K to 300 K while the GaAs LED had a shift. In 2010, the 986 nm photo-pumped GaAsBi/GaAs Fabry–Perot (FP) cavity lasers were achieved by molecular beam epitaxy (MBE).[5] Three years later, the wavelength was extended to 1204 nm by the same research group.[6] The characteristic temperature

---

[a] shumin@mail.sim.ac.cn
[b] yyli@mail.sim.ac.cn

© Author(s) 2017

(T_0) was 100 K in the range from 20 °C to 80 °C which is larger than that of the 1.3 µm InGaAsP FP-LDs, and the temperature coefficient of lasing wavelength was only 40% of that of the 1.3 µm InGaAsP FP-LDs. Ludewig *et al.* realized the first electrically pumped GaAsBi/GaAs single quantum well (QW) LD with the wavelength of 947 nm at room temperature (RT).[7] Soon, Yoshimoto *et al.* extended the wavelength to 1045 nm with up to 4% Bi in a single GaAsBi/GaAs QW grown by MBE.[8] Recently, GaAsBi/GaAs multiple QW LDs have been fabricated with a wavelength of 1060 nm at RT.[9] In this letter, we present data of electrically pumped GaAs/GaAsBi LDs emitting at 1141 nm at RT. The device structures were grown by MBE at 375 °C. Under pulsed excitation, cavity-length dependent LDs were measured and device parameters including transparent current density, internal loss and internal quantum efficiency were extracted. We have demonstrated the maximum lasing temperature up to 273 K under the continuous wave (CW) excitation. The characteristic temperature are extracted to be 125 K in the temperature range of 77~150 K, and reduced to 90 K in the range of 150~273 K. The temperature coefficient of 0.3 nm/K is extracted in the temperature range of 77~273 K.

EXPERIMENT

Laser samples were grown by DCA P600 solid source MBE on *n*-doped GaAs (001) substrates with the structure shown in Fig. 1. The 15 nm GaAsBi QW is embedded by 40 nm GaAs plus 160 nm grading layer AlGaAs with the increasing Al component from 0.2 to 0.35 to confine carriers. The active region was grown at 375 °C for effective incorporation of Bi. Both the *n*-type and *p*-type AlGaAs

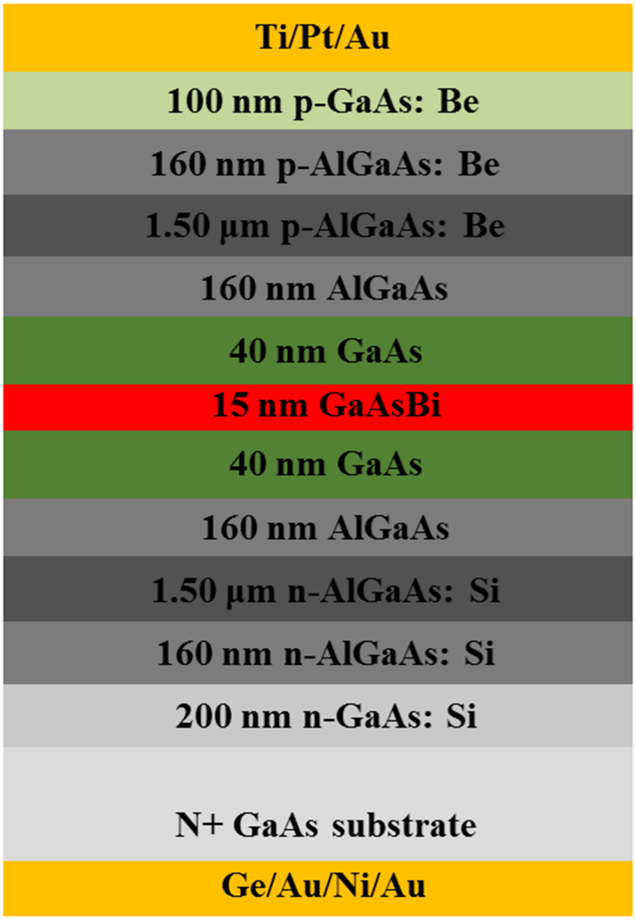
Ti/Pt/Au
100 nm p-GaAs: Be
160 nm p-AlGaAs: Be
1.50 µm p-AlGaAs: Be
160 nm AlGaAs
40 nm GaAs
15 nm GaAsBi
40 nm GaAs
160 nm AlGaAs
1.50 µm n-AlGaAs: Si
160 nm n-AlGaAs: Si
200 nm n-GaAs: Si
N+ GaAs substrate
Ge/Au/Ni/Au

FIG. 1. Structure of GaAsBi QW LD.

waveguide layers for restraint of light are 1.5 μm thick at a doping level of 1×10^{17} cm^{-3} by silicon (Si) and 1×10^{18} cm^{-3} by beryllium (Be), respectively. The grading layers are 160 nm *n*-AlGaAs:Si (1×10^{18} cm^{-3}) and *p*-AlGaAs:Be (5×10^{18} cm^{-3}) with the change in the Al component between 0.35 and 0.2. A 100 nm thick p^+-GaAs:Be (3×10^{19} cm^{-3}) layer was grown on top of the structure for making an Ohmic contact. For device fabrication, firstly a mixed solution of $H_3PO_4/H_2O_2/H_2O$ was used to etch the laser bar at the width of 6-12 μm to the upper waveguide layer at RT. After forming a strip, a 250 nm thick SiN passivation layer was deposited by inductively coupled plasma chemical vapor deposition on the bars. Then, Ti/Pt/Au electrodes were achieved by electron beam evaporation on top of the *p*-type contact layer and Ge/Au/Ni/Au-based contact was deposited on the substrate backside after the substrate was thinned to about 120 μm. To form a good Ohmic contact, annealing at a temperature of 370 °C for 40 seconds was used. Since the devices were grown on GaAs substrates, standard techniques were adopted to cleave the laser facets with different lengths. Device measurements at RT were executed on a temperature controllable probe station. An optical spectrum analyzer and an InGaAs photodiode optical power meter were employed to detect spectrum and output power. Pulsed mode measurements with a 200 ns pulse width and a 50 KHz repetition rate were used to avoid heating effect. Measurements in the CW mode were also adopted to analyze LD performance.

RESULTS AND DISCUSSION

Fig. 2 depicts both voltage-current (V-I) and output power-current (P-I) curves for the GaAsBi/GaAs QW LD with a cavity length of 1600 μm under pulsed condition at 300 K. When the current reached the threshold, the optical power increased significantly. Clear lasing behavior was observed with increasing the injected current as evidence from the P-I curve. The threshold current (I_{th}) is 435 mA, giving a threshold current density (J_{th}) of 4.54 kA/cm^2. Compared with the 1060 nm lasers grown jointly by MBE and MOVPE (J_{th}=25 kA/cm^2),[3] the threshold current density is significantly reduced. This could be attributed mainly to the optimization of MBE growth, which effectively suppresses impurities and defects and reduces the non-radiative recombination center. High structural quality of the samples was confirmed by means of transmission electron microscopy (TEM) (not shown here). The interfaces of QW in the GaAsBi/GaAs active zone were smooth and no significant extended defects, clustering or contrast modulations detected. However, compared with the conventional III-V GaAs/AlGaAs lasers the J_{th} was still relatively higher.[10] Marko *et al.* reported the lowest J_{th} for a single AlGaAs/GaAsBi QW by optimizing the Al% in the AlGaAs barriers.[11] The J_{th} can be reduced from 7.5 kA/cm^2 to 1 kA/cm^2 through increasing the Al% from 0% to 12% at RT. A higher Al fraction in the barriers benefits the confinement of electrons. However, it reduces the optical confinement factor and causes decrease in modal gain.

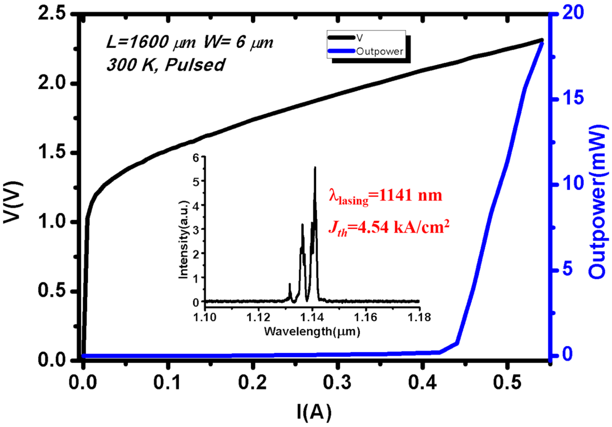

FIG. 2. P-I and V-I curves of a GaAsBi/GaAs QW LD at 300 K with a cavity length of 1600 μm under pulsed mode. The inset shows the lasing spectrum at $1.2I_{th}$.

The relatively high J_{th} in our devices may be attributed to the less confinement of the GaAs/GaAsBi structures for electrons. The conduction band offset between GaAsBi and GaAs is too small because Bi mainly affects the valence band of GaAs. Besides, inhomogeneous Bi distribution in the active layer is also responsible for the relatively high J_{th} values, which will be discussed below. For the emission spectrum, conspicuous narrowing and threshold lasing accompanied with the increasing drive current were observed, proving from spontaneous to a stimulated emission of a laser action. The inset presents the corresponding lasing spectrum recorded at $1.2I_{th}$. The center wavelength is 1141 nm with up to 5.8% Bi extracted by high-resolution X-ray diffraction as well as the bandgap of $GaAs_{1\text{-}x}Bi_x$.

To characterize device performances in detail, spontaneous emission (SE) under CW mode and photoluminescence (PL) of the SQW device at RT are presented in Fig. 3(a). For the SE performance, the device exhibits a single SE peak which is similar to other reported devices.[11] As the injected current increases from 50 to 300 mA, the spectrum displays a small blue shift of 20 nm from 1.15 μm to 1.13 μm due to the increased contribution from the higher energy states, accompanied with broadening of the SE line-width. The full width at half maximum (FWHM) of SE at low current is ~84 meV, which is larger than kT (where k is the Boltzmann constant). This indicates a degree of inhomogeneity of the carrier distribution in the active area. For the PL spectrum, we etched the device structures to the upper confined AlGaAs layer for better characterization. A single asymmetric PL spectrum at 1.02 eV with low-energy tail is observed. As suggested by Buyanova *et al.*[12] this form of PL emission can be explained by the recombination of excitons trapped by potential oscillation induced by random composition distribution at the band edge which has also been reported for GaNAs/GaAs QW.[13] The peak wavelength was 1.22 μm, longer than that of the SE spectrum. This can be explained by reabsorption effect when photons propagate along the device structure.[3] The FWHM of PL broadens to 124 meV at RT, which further proves the inhomogeneous broadening of the active layer. This inhomogeneous broadening effect has been observed for quantum dot lasers, which are representative examples of intensely inhomogeneous devices.[14–16] For our devices, the inhomogeneous broadening may be attributed to the low temperature growth and non-uniform of the Bi fractions existing in the active area. Bi serves as a surfactant to enable a smooth growth of the subsequent GaAs growth, as well as GaAsBi growth.[17–19] Surplus Bi that segregates at the surface is undesirable and hinders the growth of uniform GaAsBi layers.[20] This relative low crystal quality will seriously facilitate the high J_{th} value, especially for the very low temperature growth of the GaAs barrier layers in the QW structure.

It is worthwhile to investigate recombination behavior in the active layer of these devices in more detail. PL spectra from the GaAs/GaAsBi QW sample at 290 K were measured under different excitation powers of a 532 nm laser diode and are represented in Fig. 3(b). The sample was stacked with 200 nm GaAs buffer, GaAs/GaAsBi/GaAs (40/15/40 nm) active layer and 160 nm AlGaAs on

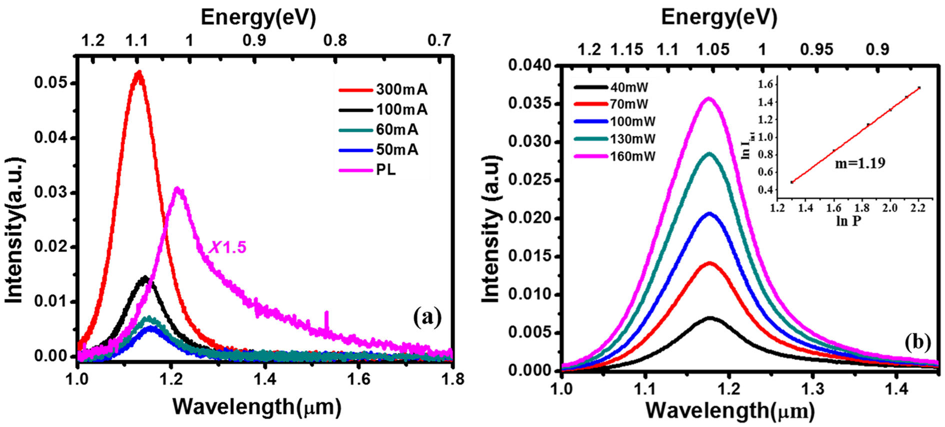

FIG. 3. (a) SE and PL spectrum for GaAsBi/GaAs QW LD device at 300 K. (b) PL spectrum for GaAsBi/GaAs QW at 290 K under different exciting power. The inset shows linear fitting of ln I_{int} and ln P.

the GaAs substrate. The QW had the same growth condition as the device active layer. The sample displays an obvious emission at RT indicating that the active layer material has a relatively desirable quality. As the exciting power is changed from 40 to 160 mW, the PL spectrum peak intensity linearly increases. The FWHM is also proportional to the exciting power and symmetrically broadened from 88.9 to 104.3 meV for the same reason as discussed above. The peak energy is essentially independent of excitation power under the moderate optical excitation level suggesting that a band-to-band transition of the QW. Void of blue shift at RT for QW structure could be due to negligible effect of band-bending and band-filling, because of good quality GaAsBi/GaAs active layer, with lower fluctuations of electrostatic potential as a result of optimized growth conditions.[21] It has been proved that the qualitative relationship of the different recombination processes in materials can be effectively obtained through the integral intensity evolution of the PL spectrum and the photo-generated carrier density, n.[22,23] There are three main recombination mechanisms of the photo-generated carrier: (1) Shockley-Read-Hall (SRH) non-radiative recombination, (2) radiative recombination, and (3) Auger recombination. The PL integrated intensity can be well described by the equation $I_{\text{int}} \propto P^m$, where I_{int} is the PL integrated intensity, and P is the excited power. When m is equal to *1, 2* or *2/3,* it corresponds to radiation recombination, SRH non-radiative recombination or Auger recombination mechanism,[24] respectively. Analysis of the GaAsBi/GaAs QW data based on the inset of Fig. 3(b) yields an m of 1.19. This result indicates that the dominant carrier recombination mechanism is radiative with small defect induced non-radiative recombination at 290 K.

Fig. 4(a) shows the inverse of the external differential quantum efficiency ($1/\eta_d$) as a function of the cavity length (L) of the LDs at 300 K under the pulsed condition. $1/\eta_d$ is related to the cavity length according to Equation 1 presented below, where η_i, R and α_i are the internal quantum efficiency, the reflectivity of the mirror and the internal optical loss, respectively. From Equation 1 η_i and α_i are derived to be 86% and 10 cm^{-1}, respectively, while the loss at two facets between air and the mirror is about 8 cm^{-1} for the device with the cavity length of 1600 µm. η_i indicates the percentage of electrically injected carriers reaching to the GaAsBi/GaAs QW active region, which is important to evaluate the material quality. This high value for GaAsBi LD is inspiring particularly for this relative high Bi composition LDs. But compared with the conventional III-V GaAs/AlGaAs,[25] GaInNAs[26] QW LDs and even InGaAs/GaAs quantum dots LDs[27] etc., this value for GaAsBi materials still need to be further improved by e.g. rapid thermal annealing to optimize the optical performance and reduce localized defects. The α_i results from free carrier absorption in the active layer and doped AlGaAs waveguide layers. Therefore, further improvement could be achieved by optimizing the doping concentration and profile of the waveguide layers or increasing the waveguide thickness. Fig. 4(b) plots the $\ln(\eta_i J_{th})$ against the inverse of the cavity length at 300 K under pulsed condition. The relationship of $\ln(\eta_i J_{th})$ and $1/L$ can be characterized by Equation 2,[28–31] where Γ is the optical confinement factor calculated by COMSOL Multiphysics simulation software with wave optics module and g_0 is the gain coefficient. For the design of this structure, Γ is 1.22% as calculated by COMSOL Multiphysics simulation software with wave optics module. From the plot and the linear fitting curve, the transparency current density J_{tr} is determined to be 196 A/cm^2. $J_{tr}$is

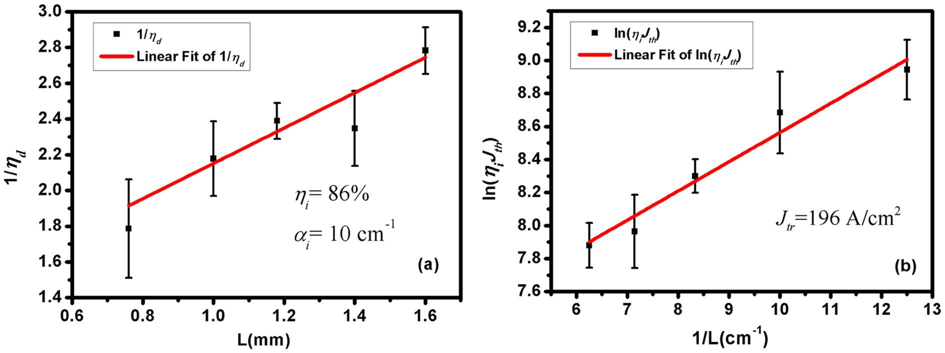

FIG. 4. (a) Inverse of external differential quantum efficiency against cavity length of LDs at 300 K and (b) Logarithmic of $\eta_i J_{th}$ against inverse of the cavity length of LDs at 300 K under pulsed condition.

the minimal current density for the materials to become transparent and not absorb any photon energy when the photon energy is larger than or equal to the bandgap of GaAs/GaAsBi QW. It is closely related to material quality: defects and some other sources of non-radiative recombination.[32]

$$\frac{1}{\eta_d} = \frac{\alpha_i}{\eta_i \text{In}(1/R)} L + \frac{1}{\eta_i} \tag{1}$$

$$\text{In}(\eta_{\text{i}} J_{th}) = \frac{\text{In}(1/\text{R})}{\Gamma g_0} \times \frac{1}{L} + \left(\frac{1}{\Gamma g_0} a_i + \text{In}\, J_{tr} \right). \tag{2}$$

Fig. 5(a) (b) and (c) illustrate the performances of the LDs under CW mode at temperature ranging from 77 to 273 K with a cavity length of 1500 µm and width of 6 µm. From the P-I curves at different temperatures as presented in Fig. 5(a), it can be noted that the highest working temperature for the LDs was 273 K in CW mode. The devices yield the wavelength of 1.135 µm and the J_{th} of 5.5 kA/cm^2 under the CW mode at 273 K. The J_{th} value is a little larger than the pulsed mode under 300 K because of the thermal effect. The characteristic temperature (T_0) of J_{th} is found to be 125 K at the temperature range of 77~150 K and deceased to 90 K at the temperature range of 150~273 K deduced from the equation $I_{th} = I_0 \exp(\text{T/T}_0)$ as illustrated in Fig. 5(b), which were comparable to the reported optically pumped 1204 nm GaAsBi LD (T_0=90 K)[6] and the electrically injected (T_0=90 K)[9] 1060 nm GaAsBi LDs, but obviously larger than the typical WDM InGaAsP/InP LDs (T_0=60 K). The decrement of T_0 with increasing temperature is a result of a combination of many reasons:[3] carrier leakage due to the lack of effective electron confinement, thermally-related carrier redistribution behavior, as well as activation of non-radiative recombination attributed to the non-uniform Bi composition in the active region. It is worth noting that the value of T_0 is similar to the previously reported GaAsBi lasers (T_0=90~125 K), indicating T_0 may be independent of Bi composition.[33] For the previously mentioned QW lasers of optimized 12% Al in barrier layer T_0 is equal to 100 K above RT.[11] This indicates that the low T_0 for GaAsBi LDs was mainly due to the non-radiative recombination caused by Bi-related defects. Fig. 5(c) presents lasing wavelength

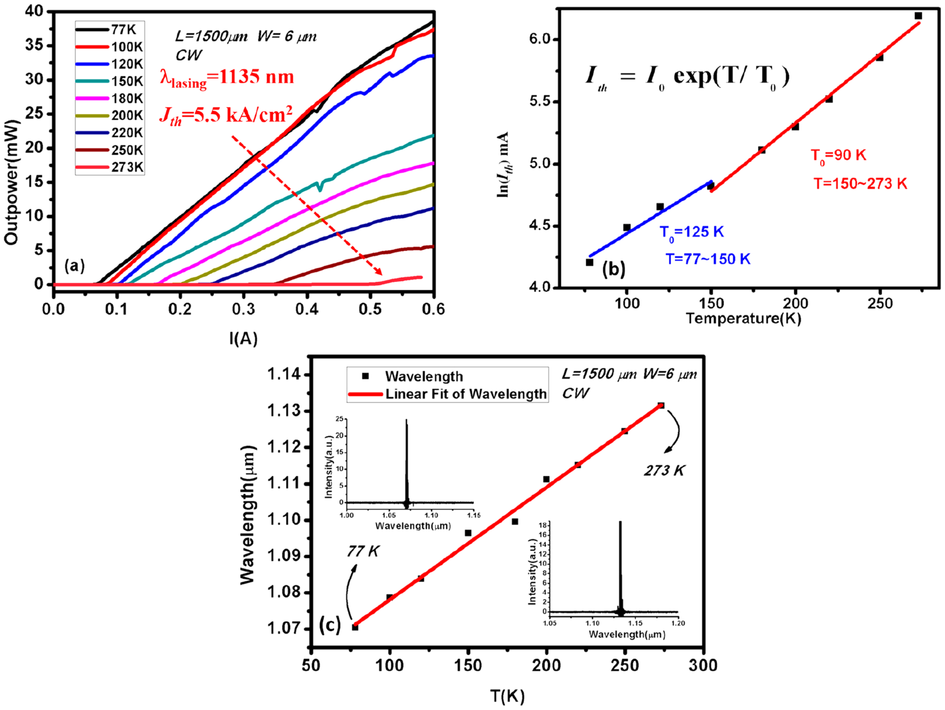

FIG. 5. (a) P-I curves of a GaAsBi/GaAs QW LD, (b) Temperature dependence of the threshold current and (c) Lasing wavelength against temperature for a 1500x6 µm^2 cavity under CW mode at the temperature range of 77~273 K.

at different temperatures. From the linear fitting curve, the temperature coefficient is deduced to be 0.3 nm/K (or 0.317 meV/K), which is lower than that of GaAs (0.56 meV/K) and InGaAsP (0.45 nm/K) system. The reduction is related to the temperature insensitive bandgap of GaAsBi due to the resonance between the Bi impurity band with the valence band of GaAsBi. This result suggests that GaAsBi LDs have potential applications in future uncooled semiconductor LDs in information and communication technology.

CONCLUSION

In summary, we demonstrate electrically injected GaAsBi/GaAs QW LDs with lasing wavelength extended to 1141 nm at 300 K under pulsed mode. From the cavity length dependent measurements, the internal quantum efficiency and the optical loss are deduced to be 86% and 10 cm^{-1}, respectively. The GaAsBi/GaAs QW LDs is operable under CW mode up to 273 K, and the characteristic temperature are extracted to be 125 K in the temperature range of 77~150 K, and reduced to 90 K in the range of 150~273 K. The temperature coefficient of 0.3 nm/K is extracted in the temperature range of 77~273 K. These results clearly indicate that the GaAsBi LD is promising as a candidate for near infrared optical telecommunication lasers.

ACKNOWLEDGMENTS

This work was financially supported by the Key Program of Natural Science Foundation of China (Grant No. 61334004), the National Basic Research Program of China (Grant No. 2014CB643902), the Natural Science Foundation of China (Grant No. 61404152), the foundation of the National Laboratory for Infrared Physics, Shanghai Institute of Technical Physics of the Chinese Academy of Sciences and the Swedish Research Council (VR).

[1] L. Wang, L. Zhang, L. Yue, D. Liang, X. Chen, Y. Li, P. Lu, J. Shao, and S. Wang, Crystals **7**, 63 (2017).
[2] S. Jin and S. John Sweeney, J. Appl. Phys. **114**, 213103 (2013).
[3] I. P. Marko, S. R. Jin, K. Hild, Z. Batool, Z. L. Bushell, P. Ludewig, W. Stolz, K. Volz, R. Butkutė, V. Pačebutas, A. Geizutis, A. Krotkus, and S. J. Sweeney, Semicond. Sci. Technol. **30**, 094008 (2015).
[4] R. B. Lewis, D. A. Beaton, X. Lu, and T. Tiedje, J. Cryst. Growth **311**, 1872 (2009).
[5] Y. Tominaga, K. Oe, and M. Yoshimoto, Appl. Phys. Express **3**, 62201 (2010).
[6] T. Fuyuki, R. Yoshioka, K. Yoshida, and M. Yoshimoto, Appl. Phys. Lett. **103**, 202105 (2013).
[7] P. Ludewig, N. Knaub, N. Hossain, S. Reinhard, L. Nattermann, I. P. Marko, S. R. Jin, K. Hild, S. Chatterjee, W. Stolz *et al.*, Appl. Phys. Lett. **102**, 242115 (2013).
[8] T. Fuyuki, K. Yoshida, R. Yoshioka, and M. Yoshimoto, Appl. Phys. Express **7**, 082101 (2014).
[9] R. Butkute, A. Geižutis, V. Pačebutas, B. Cechavičius, P. Ludewig, V. Bukauskas, R. Kundrotas, K. Volz, and A. Krotkus, Electron. Lett. **50**, 1155 (2014).
[10] S. Miyazawa, Y. Sekiguchi, and N. Mizutani, Jpn. J. Appl. Phys. **30**, L1935 (1991).
[11] I. P. Marko, P. Ludewig, Z. L. Bushell, S. R. Jin, K. Hild, Z. Batool, S. Reinhard, L. Nattermann, W. Stolz, K. Volz *et al.*, J. Phys. D. Appl. Phys. **47**, 345103 (2014).
[12] I. A. Buyanova, W. M. Chen, G. Pozina, J. P. Bergman, B. Monemar, H. P. Xin, and C. W. Tu, Appl. Phys. Lett. **75**, 501 (1999).
[13] X. D. Luo, Z. Y. Xu, W. K. Ge, Z. Pan, L. H. Li, and Y. W. Lin, Appl. Phys. Lett. **79**, 958 (2001).
[14] I. P. Marko, N. F. Massé, S. J. Sweeney, A. D. Andreev, A. R. Adams, N. Hatori, and M. Sugawara, Appl. Phys. Lett. **87**, 211114 (2005).
[15] M. T. Crowley, I. P. Marko, N. F. Masse, A. D. Andreev, S. Tomic, S. J. Sweeney, E. P. O'Reilly, and A. R. Adams, IEEE J. Sel. Top. Quantum Electron. **15**, 799 (2009).
[16] I. P. Marko, A. D. Andreev, A. R. Adams, R. Krebs, J. P. Reithmaier, and A. Forchel, IEEE J. Sel. Top. Quantum Electron. **9**, 1300 (2003).
[17] F. Bastiman, A. G. Cullis, J. P. R. David, and S. J. Sweeney, J. Cryst. Growth **341**, 19 (2012).
[18] G. Vardar, S. W. Paleg, M. V. Warren, M. Kang, S. Jeon, and R. S. Goldman, Appl. Phys. Lett. **102**, 42106 (2013).
[19] D. Fan, P. C. Grant, S. Q. Yu, V. G. Dorogan, X. Hu, Z. Zeng, C. Li, M. E. Hawkridge, M. Benamara, and Y. I. Mazur *et al.*, J. Vac. Sci. Technol. B Microelectron. Nanom. Struct. **31**, 03C105 (2013).
[20] P. Ludewig, N. Knaub, W. Stolz, and K. Volz, J. Cryst. Growth **370**, 186 (2013).
[21] Y. G. Sadofyev and N. Samal, Materials (Basel) **3**, 1497 (2010).
[22] N. A. Riordan, C. Gogineni, S. R. Johnson, X. Lu, T. Tiedje, D. Ding, Y. H. Zhang, R. Fritz, K. Kolata, S. Chatterjee *et al.*, J. Mater. Sci. Mater. Electron. **23**, 1799 (2012).
[23] I. P. Seetoh, C. B. Soh, E. A. Fitzgerald, and S. J. Chua, Appl. Phys. Lett. **102**, 101112 (2013).
[24] X. D. Luo, P. H. Tan, Z. Y. Xu, and W. K. Ge, J. Appl. Phys. **94**, 4863 (2003).
[25] I. Schnitzer, E. Yablonovitch, C. Caneau, and T. J. Gmitter, Appl. Phys. Lett. **62**, 131 (1993).
[26] H. Zhao, G. Adolfsson, S. M. Wang, M. Sadeghi, and A. Larsson, Electron. Lett. **44**, 475 (2008).

[27] R. L. Sellin, C. Ribbat, M. Grundmann, N. N. Ledentsov, and D. Bimberg, Appl. Phys. Lett. **78**, 1207 (2001).
[28] S. L. Chuang, *Physics of Optoelectronic Devices* (Wiley, New York, 1995), Chap. 10, 434.
[29] S. M. Sze and K. K. Ng, *Physics of Semiconductor Devices* (John Wiley &Sons, New Jersey, 2007), Chap. 12, 640.
[30] C. Y. Liu, S. F. Yoon, Q. Cao, C. Z. Tong, and H. F. Li, Appl. Phys. Lett. **90**, 041103 (2007).
[31] H. K. Choi and C. A. Wang, Appl. Phys. Lett. **57**, 321 (1990).
[32] G. Pakulski and J. Gupta, Photonics North 2004 **5577** 82 (2004).
[33] I. Marko and S. J. Sweeney, IEEE J. Sel. Top. Quantum Electron. **23**, 1501512 (2017).